Free Radical Biology & Medicine 51 (2011) 1656–1665

Contents lists available at ScienceDirect

Free Radical Biology & Medicine

journal homepage: www.elsevier.com/locate/freeradbiomed

Original Contribution

Role of oxidative stress in lysosomal membrane permeabilization and apoptosis induced by gentamicin, an aminoglycoside antibiotic

Sophie Denamur [a,1], Donatienne Tyteca [b,1], Jacqueline Marchand-Brynaert [c], Françoise Van Bambeke [a], Paul M. Tulkens [a], Pierre J. Courtoy [b,1], Marie-Paule Mingeot-Leclercq [a,*,1]

[a] Université catholique de Louvain, Louvain Drug Research Institute, Laboratory of Cellular and Molecular Pharmacology, UCL B1.73.05, avenue E. Mounier 73, B-1200 Bruxelles, Belgium
[b] Université catholique de Louvain, de Duve Institute, Laboratory of Cell Biology, UCL B1.75.02, avenue Hippocrate 75, B-1200 Bruxelles, Belgium
[c] Université catholique de Louvain, Institute of Condensed Matter and Nanosciences, Laboratory of Solids, Molecules and Reactivity, UCL L4.01.02, Place Louis Pasteur 1, B-1348 Louvain-la-Neuve, Belgium

ARTICLE INFO

Article history:
Received 11 September 2010
Revised 8 July 2011
Accepted 16 July 2011
Available online 23 July 2011

Keywords:
Gentamicin
ROS
Deferoxamine
Membrane
Permeability
Apoptosis
Free radicals

ABSTRACT

Gentamicin, an aminoglycoside antibiotic used to treat severe bacterial infections, may cause acute renal failure. At therapeutic concentrations, gentamicin accumulates in lysosomes and induces apoptosis in kidney proximal tubular cells. In gentamicin-treated renal LLC-PK1 cells, acridine orange release from lysosomes, previously interpreted as lysosomal membrane permeabilization, precedes the apoptotic cascade that develops during incubation with gentamicin. However, the link between gentamicin lysosomal accumulation and apoptosis remains unclear. We here examined if reactive oxygen species (ROS) production could account for gentamicin-induced acridine orange release and apoptosis, and the implication of iron in these events. We found that gentamicin induced ROS production prior to, and at lower drug concentrations than required for, acridine orange release and apoptosis. ROS antioxidant or scavenger, catalase, and *N*-acetylcysteine largely prevented these events. Vital confocal imaging revealed that gentamicin-induced ROS production occurs in lysosomes. Deferoxamine, an iron chelator, which is endocytosed and accumulates in lysosomes, largely prevented gentamicin-induced ROS production as well as apoptosis. Direct evidence for gentamicin-induced permeabilization of lysosomal membrane was provided by showing the release into the cytosol of Lucifer yellow, a membrane-impermeant endocytic tracer with a comparable molecular weight as gentamicin. Altogether, our data demonstrate a key role of lysosomal iron and early ROS production in gentamicin-induced lysosomal membrane permeabilization and apoptosis.

Aminoglycosides including gentamicin have been successfully used for decades in the treatment of Gram-negative bacterial infections [1,2] and currently regain popularity because of widespread resistance to other antibiotic classes [3,4]. Unless careful serum monitoring and optimized administration, aminoglycosides can, however, induce acute nephrotoxicity in 5–25% of treated patients, and even more in populations at risk [2]. Nephrotoxicity induced by gentamicin is due to uptake of the ultrafiltrated polycationic drug by proximal tubular cells, via adsorptive/ receptor-mediated endocytosis upon binding to acidic phospholipids and megalin at the brush border [5,6]. As a result, gentamicin accumulates to large extent in lysosomes [7], although cell culture studies suggest a way to the cytosol by retrograde transport via the Golgi complex and the endoplasmic reticulum [8]. Accumulation of gentamicin in proximal tubular cells rapidly leads to lysosomal phospholipidosis, due to inhibition of acid phospholipases, followed by mixed apoptosis/necrosis together with signs of tubular regeneration/peritubular inflammation and fibrosis that ultimately lead to renal dysfunction (see review in [9]).

Apoptosis induced by aminoglycosides can be reproduced *in vitro* using cells of both renal (LLC-PK1 and MDCK) and non-renal (fibroblasts) origin and correlates with the level of drug accumulation [10]. One mechanism proposed to link aminoglycoside lysosomal accumulation with apoptosis is permeabilization of the lysosomal membrane based on change in the fluorescence emission of acridine orange. In LLC-PK1 cells [11], this shift is already detectable after 2 h of drug exposure, increases over time and precedes appearance of other changes directly related to apoptosis triggering and execution, including loss of mitochondrial potential, release of cytochrome *c* and activation of caspase-9 [11]. That permeabilization of lysosomes causing release of gentamicin into the cytosol may trigger apoptosis is supported by direct cytosolic introduction of the antibiotic via electroporation [12]. Cytosolic gentamicin could either act directly on mitochondria by causing the release of intermembrane proteins, as shown for a variety of polycations including aminoglycosides [13], or indirectly through impairment of Bax proteosomal degradation [12] upon drug binding to the β-9 proteasome subunit [14]. Alternatively,

* Corresponding author. Fax: +32 2 764 73 73.
E-mail address: marie-paule.mingeot@uclouvain.be (M.-P. Mingeot-Leclercq).
[1] These authors contributed equally to this work.

0891-5849/$ – see front matter © 2011 Elsevier Inc. All rights reserved.
doi:10.1016/j.freeradbiomed.2011.07.015

apoptosis could also be triggered by lysosomal release of cysteine- and aspartyl-cathepsins, known to directly activate cell death signaling pathways [15,16].

Lysosomal membrane permeabilization by gentamicin remains, however, hypothetical and its mechanism is obscure. A simple explanation invokes membrane destabilization upon drug binding to the inner luminal leaflet phospholipids [17], which would be favored by the acidic pH [11]. However, several observations point to a role of reactive oxygen species (ROS) in this process. Indeed, lysosomes generally contain a high iron pool [18,19] which, combined with a reducing potential and acidic pH [20], should favor ROS production. This reaction could be enhanced by gentamicin when forming a ternary complex with iron and membrane phosphoinositides [21].

In the present study, we have first examined the induction by gentamicin of ROS production in the kidney proximal tubular cells-derived cell line, LLC-PK1. We next assessed their role, as well as that of iron, in triggering lysosomal membrane destabilization and cell apoptosis by using antioxidants and deferoxamine. Given the importance of lysosomal permeabilization to the proposed model as well as the concerns raised by change in the fluorescence emission of acridine orange release for studying lysosomal membrane permeabilization, we also documented this critical event by following the release of the membrane bilayer-impermeant lysosomal vital tracer, Lucifer yellow. Of interest, the molecular weight of Lucifer yellow is comparable to that of gentamin. Our results demonstrate a role for ROS in a cascade linking gentamicin lysosomal accumulation and membrane permeabilization with apoptosis.

Materials and methods

Materials

Dulbecco's Modified Eagle's Medium (DMEM) and trypsin-EDTA were purchased from Life Technologies, Paisley, UK. Gentamicin sulfate (GEOMYCINE®) was from GlaxoSmithKline, Belgium. 4',6'-diamidine-2'-phenylindole (DAPI) was from Roche (Basel, Switzerland). Acridine orange, bafilomycin A1, catalase, deferoxamine (DFO), 1,4-diazabicyclo [2.2.2]octane (DABCO), Lucifer yellow, monensin, *N*-acetylcysteine and probenecid were from Sigma-Aldrich (St-Louis, MO, USA). 2',7'-dichlorodihydrofluorescein diacetate (H_2DCFDA), MitoTracker Deep Red and LysoTracker Red were from Invitrogen (Paisley, UK). Unless stated otherwise, all other reagents were of analytic grade and purchased from Merck (Darmstadt, Germany).

Cells and gentamicin incubation

All experiments were performed with LLC-PK1 cells (Lilly Laboratories, Culture-Pig Kidney Type 1) from ATCC (CL-101). This cell line was isolated from, and displays some attributes of kidney proximal tubular cells [22]. Cells were cultivated in DMEM supplemented with 10% foetal calf serum (FCS) in 95% air - 5% CO_2. They were subcultured twice a week and used at ~80% confluence. All gentamicin solutions were adjusted to pH 7.4 prior addition to the culture medium. Electroporation was performed with cells detached by trypsinization as previously described [12].

Oxidative stress assay

ROS were detected by means of the oxidation-sensitive fluorescent probe, 2',7'-dichlorodihydrofluorescein (H_2DCF). The membrane-permeant fluorigenic precursor (2',7'-dichlorodihydrofluorescein diacetate (H_2DCFDA) is deacetylated by cytosolic esterases to H_2DCF, which is further oxidized into the fluorescent compound, 2',7'-dichlorofluorescein (DCF) when and where cellular peroxides are produced [23]. In our fluorimetric experiments, cells were cultured in 96-wells microplates, rinsed, and preincubated at 37 °C for 30 min with 10 μM H_2DCFDA in Krebs-Ringer-HEPES buffer (KRH) to avoid extracellular hydrolysis of the probe. They were then incubated with the indicated compounds in Hanks'Balanced Salt Solution (HBSS), and examined at 1-h intervals with a Fluorocount Microplate Fluorometer (Packard Instrument Company, Downers Grove, IL, USA) with excitation wavelength at 485 nm and emission recorded at 530 nm.

Acridine orange release

Acridine orange is a fluorescent membrane-permeant weak base, which reversibly accumulates into acidified membrane-bound compartments [24]. The fluorescence emission of acridine orange is concentration-dependent, from red at high concentrations (e.g. in lysosomes) to green at low concentrations (e.g. in the cytosol) [24,25], with yellow as intermediate (e.g. upon trapping in nucleoli). However, fluorescence of acridine orange is also dependent of changes of pH, as reported in literature [26]. Shift in red-to-green emission ratio in comparison to controls may thus either monitor lysosomal leakage or change in lysosomal pH.

In our fluorimetric studies, cells cultured in 24-wells culture plates were first loaded with acridine orange (5 μg/mL) in DMEM with FCS at 37 °C for 15 min, rinsed, then incubated in HBSS with or without gentamicin for the indicated times. Whole cell sheets were examined at 1-h intervals with the Fluorocount Microplate Fluorometer with excitation wavelength at 485 nm and emission recorded at 530 nm and 620 nm.

Counting of apoptotic cells

Apoptotic nuclear fragmentation, revealed by DNA staining with 4',6'-diamidine-2'-phenylindole (DAPI) [11], was identified during random counting of 500 cells per condition. Clusters of apoptotic bodies were given as a single count. Data were expressed as the percentage of apoptotic nuclei relative to total number of nuclei counted.

Vital imaging of lysosomal alterations

Cells were cultured in Lab-Tek II chambers. For acridine orange labeling, cells were pre-incubated with 5 μg/mL acridine orange for 15 min, rinsed and replaced in culture medium supplemented with 10% fœtal calf serum containing 3 mM gentamicin, 100 nM bafilomycin or 50 μM monensin, for 2 or 6 hours as mentioned. Cells were briefly washed and immediately observed with a LSM 510 META confocal microscope (Zeiss, Jena, Germany) using a Plan-Apochromat 63X/1.4 oil DIC objective, with imaging in the green and red channels simultaneously.

For Lucifer yellow labeling, cells were pre-incubated with 2 mg/mL Lucifer yellow overnight (pulse), then chased for 6 hours in medium alone or supplemented by 3 mM gentamicin, 100 nM bafilomycin or 50 μM monensin. One hour before the end of this incubation, cells were rinsed with serum-free DMEM, incubated with 250 nM MitoTracker Deep Red in serum-free DMEM for 30 minutes, rinsed and reincubated in complete growth medium for 30 minutes, both steps maintaining same gentamicin, bafilomycin or monensin concentrations.

In a second part of experiments, pulse and chase were both made in absence or presence of 2.5 mM probenecid, to sensitize detection of Lucifer yellow release by preventing endosomal/lysosomal recapture and/or efflux from cytosol [27]. At the end of the chase, cells were briefly washed and immediately observed by vital imaging.

Vital imaging of oxidative stress

Cells cultured in Lab-Tek II chambers were preincubated or not for 3 hours with deferoxamine, then incubated with or without 200 μM H_2O_2 or 2 mM gentamicin for the indicated times, maintaining the same concentrations of deferoxamine. One hour before the end of this

incubation, cells were rinsed with serum-free DMEM, incubated with 250 nM MitoTracker Deep Red in serum-free DMEM for 30 minutes, rinsed and reincubated with 3 μM H_2DCFDA and 50 nM LysoTracker Red in KRH for 30 minutes. H_2O_2, gentamicin and deferoxamine were maintained up to imaging with the confocal microscope using a Plan-Apochromat 63X/1.4 oil DIC objective. Because H_2DCFDA is susceptible to photo-oxidation, images were sequentially collected in the green, red and blue channels at low laser power and with a single scan under identical conditions for all samples.

Determination of gentamicin cell content

The cellular gentamicin content was assessed by a disc-plate microbiological technique using *Bacillus subtilis* (ATCC 6633) as test

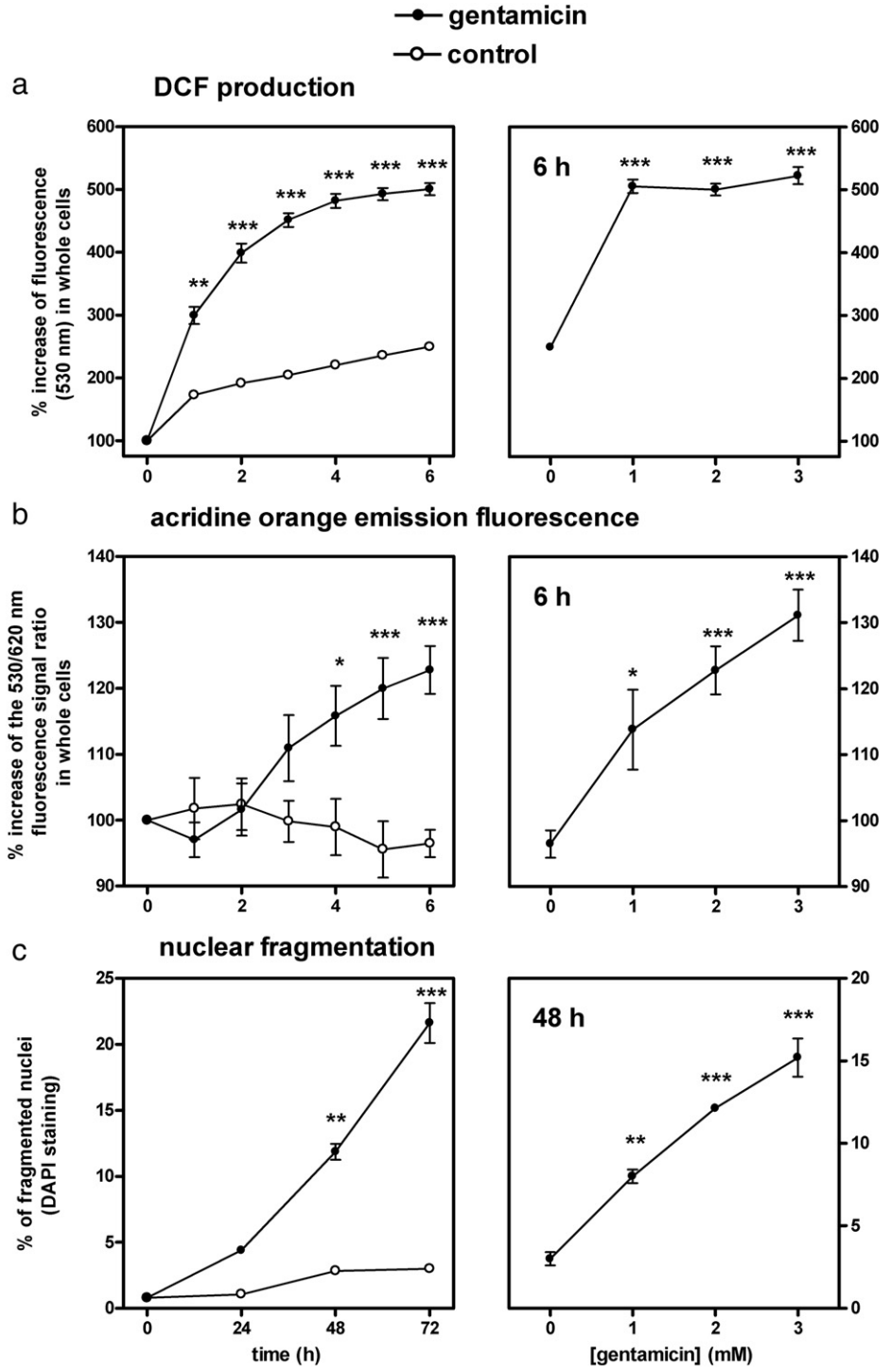

Fig. 1. Effect of gentamicin on ROS production, acridine orange emission fluorescence shift, and apoptosis in LLC-PK1 cells. Left, effect of incubation time with 2 mM gentamicin (closed symbols) as compared with untreated controls (open symbols). Right, effect of gentamicin concentration after 6 h (ROS production and acridine orange emission fluorescence shift) and after 48 h (apoptosis). Top panels. ROS production was monitored by 2',7'-dichlorofluoresceine production (DCF). Central panels. Effects on lysosomes were evaluated by the shift of acridine orange emission ratio, as percentage of value at time 0. Bottom panels. Apoptosis was measured as the percent of cells with fragmented nuclei. Data are means ± SD (n = 6 from 2 separate experiments for ROS; n = 9 from 3 separate experiments for lysosomal permeabilization; n = 3 for apoptosis; where not visible, error bars are included in the symbols).

organism [28]. Cell protein was measured by the Folin-Ciocalteu method and gentamicin cell content expressed as μg antibiotic / mg cell protein. A posteriory mixing of naive cells with defined amounts of fresh gentamicin yielded about 90% of the expected values.

Statistical analysis

All statistical analyses were perfomed with GraphPad Prism version 4.02 and GraphPad InStat version 3.06 (GraphPad Prism Software, San Diego, CA, USA). The comparison of 3 or more groups of data was performed using one-way ANOVA with Tukey's multiple comparison post-tests. The significance of the differences between two sets of data was tested using two-way ANOVA followed by Bonferroni's post-test. Paired data were compared using repeated-measures ANOVA.

Results

Gentamicin sequentially triggers ROS production, shift of acridine orange emission fluorescence and apoptosis

In a first series of experiments, we examined the time- and concentration-dependence of gentamicin-induced (i) ROS production, (ii) acridine orange emission fluorescence shift, and (iii) apoptosis. To these aims, cells were incubated with 2 mM gentamicin for increasing periods of time, or with 0–3 mM gentamicin for a fixed interval, then tested for (i) increase in fluorescence due to oxidative conversion of H_2DCF into 2,7-dichlorofluorescein (DCF); (ii) change in the ratio of the 530 to 620 nm fluorescence signals of acridine orange indicating lysosomal leakage or change in lysosomal pH; and (iii) increase in the proportion of DAPI-labeled fragmented nuclei indicating apoptosis. As shown in Fig. 1 (left panels), 2 mM gentamicin rapidly increased ROS production (half-maximal response within 1 h) to level off at 4 h (top; no further increase in fluorescence up to 8 h). Cells incubated with 200 μM H_2O_2 for 6 h, used as positive control, showed a comparable but slightly higher ROS production as upon parallel incubation with 2 mM gentamicin for the same interval (data not shown). After a lag period of ~2 h, acridine orange fluorescence emission started shifting to greener values; the green/red ratio then increased almost linearly with time (central panel; incubation for up to 24 h showed a continuous increase of the difference between gentamicin-treated and control cells (from 122 ± 2% at 6 h to 262 ± 4% at 24 h [n = 3]). Appearance of apoptotic cells was further delayed, being significant after only 24 h, then increased continuously from 24 to 72 h (bottom). These three events occurred thus sequentially. The right panels of Fig. 1 show that ROS production measured at 6 h (top) was maximal for the lowest gentamicin concentration tested (1 mM). In contrast, 530/620 nm acridine orange fluorescence ratio, also measured at 6 h (central) was roughly proportional to concentration, as was apoptosis measured at 48 h (bottom). These data thus showed that gentamicin-induced ROS production occurred both prior to, and at lower drug concentrations than the 530/620 nm ratio shift of acridine orange emission fluorescence, used as a marker of lysosomal alteration, itself followed by nuclear fragmentation reflecting apoptosis.

Gentamicin induces the release of Lucifer yellow

Although acridine orange is widely used as a marker of lysosomal "permeabilization", recognized by a decrease in red acridine orange fluorescence while maintaining high green fluorescence [29], the reversion of acidotropic sequestration due to change of pH across a still unpermeable membrane remains an alternative explanation. This possibility was tested by vital imaging using two well-established procedures to collapse lysosomal acidic pH : bafilomycin A1 and monensin. Furthermore, to avoid confusion between a change in lysosomal pH and true leakage, we followed lysosomal membrane permeabilization by vital imaging after loading cells with the pH-insensitive membrane bilayer-*impermeant* lysosomal vital tracer, Lucifer yellow (LY). The sensitivity of this approach was greatly increased by inhibiting the organic anion transporter with probenecid, as originally reported by Steinberg and his colleagues [30].

When lysosomes had been loaded by acridine orange, collapsing lysosomal pH by bafilomycin A1 (100 nM for 2 h), an inhibitor of the vacuolar proton-pump [31], or monensin (50 μM for 2 h), an electro-neutral ionophore [32], caused the virtual disappearance of dotty red signal, with full relocation of acridine orange as green signal into the cytosol, nucleosol and especially nucleoli (compare at Fig. 2, panels c, d *vs* a) whereas Lucifer yellow remained fully trapped in lysosomes (Fig. 2, panels g, h) demonstrating their integrity.

Thus, shift of red to green does not necessarily reflect lysosomal rupture and should be used with caution. Upon gentamicin treatment, lysosomes remained labelled by acridine orange, but partial relocation to nucleoli was obvious, revealing release from preloaded lysosomes and preferential trapping in nucleoli as a sensitive read-out (compare Fig. 2b *vs* Fig. 2a).

This result is consistent with either partial membrane leakage, a discrete change in lysosomal pH, or even conceivably trapping into a modified lysosomal matrix. To circumvent these undertainties, we turned our attention to Lucifer yellow, a bona fide membrane-impermeant lysosomal tracer.

Upon gentamicin treatment, we noticed that lysosomes loaded with Lucifer yellow were more clustered (Fig. 2, panel f *vs* e). When carefully examined, clusters frequently showed fuzzy boundaries, first suggesting acute Lucifer yellow release, with rapid dilution in the cytosol (Fig. 2, panel f, arrows). The X-Z series shown in Supplementary Fig. 1 suggested that the fuzzy boundaries were not artefacts due to fluorescence generated by voxels above or below the center of the focal plane.

To sensitize detection of Lucifer yellow release, we used probenecid, a well-established inhibitor of general organic anion transporters, which will prevent Lucifer yellow transfer across membranes [27,30]. As a control, we used Mitotracker to test if mitochondria could be affected in cells where ROS was induced (see Fig. 1a). We found no change in distribution and abundance of labeled mitochondria, in contrast to lysosomes (compare at Fig. 2, panels j *vs* i).

Under these conditions, cytosolic labeling by Lucifer yellow upon gentamicin treatment became prominent in a large fraction of cells (Fig. 2, panel j), whereas it was never observed upon lysosomal pH neutralization (Fig. 2 panels k,l). This set of data provides the first visual evidence that gentamicin is able to permeabilize membranes in living cells as to release small molecular weight tracers of the size of gentamicin. The reversibility of the effect of probenecid is shown in Supplementary Fig. 2.

ROS induced by gentamicin are localized in lysosomes

To test whether gentamicin-induced oxidative stress was specifically localized into lysosomes, ROS production was analyzed by vital confocal imaging based on H_2DCF conversion after lysosomal labeling with LysoTracker [in red] and mitochondria labeling with MitoTracker [in blue]. H_2O_2 was used as a control for mitochondrial ROS production. As shown in Fig. 3, lysosomes and mitochondria were clearly resolved from one another and no detection of DCF could be detected in control cells (no gentamicin added; upper row). When H_2O_2 was added (2^d row), a marked green staining appeared, which largely co-localized with mitochondria but not with lysosomes (see inset in merge). When cells had been incubated with gentamicin (lower three rows), green staining appeared instead in lysosomes, at the exclusion of mitochondria (see inset in merges). In situ imaging of ROS production in lysosomes was already obvious within 1 h of exposure to gentamicin, matching fluorimetric results of Fig. 1, increased after 6 h but decreased after prolonged incubation with gentamicin (18 h). At this late interval, while ROS and MitoTracker were never found to colocalize upon gentamicin treatment,

MitoTracker signal had completely vanished (lowest row), pointing to membrane potential perturbation and providing indirect evidence for a secondary role of mitochondria in apoptosis induced by gentamicin, as previously reported [11]. These morphological analyses indicated a sequence of organelle-specific perturbations: lysosomal ROS production, followed by a much delayed mitochondrial loss-of-function.

Antioxidant treatments largely prevent gentamicin-induced ROS production and partially protect against apoptosis

To test for a causal role of ROS in lysosomal membrane permeabilization, we next examined if pretreating cells with catalase or *N*-acetylcysteine as ROS scavengers in lysosomes could prevent gentamicin-induced ROS production, thereby conferring protection against lysosomal permeabilization and apoptosis. This set of experiments was conducted with 2 mM gentamicin, 1,000 U/mL catalase and 1 mM *N*-acetylcysteine and the exposure time was selected for optimal measurement of corresponding signals for ROS and lysosomal permeabilization (6 h) or apoptosis (48 h). As shown by Fig. 4 (upper panel), gentamicin-induced ROS production was largely prevented by catalase, and essentially abrogated with *N*-acetylcysteine. These anti-oxidant treatments also partially protected against apoptosis (lower panel). This protective effect of antioxidant molecules was also demonstrated by vital imaging (Supplementary Fig. 3). Protection by antioxidants did not result from a decreased cellular accumulation of gentamicin : after 48 h with 2 mM gentamicin, the cellular concentration was 22.3 ± 3 μg / mg protein without antioxidant, 20.6 ± 4 μg / mg protein with *N*-acetylcysteine and 24.3 ± 3 μg / mg protein with catalase.

Deferoxamine partially impairs gentamicin-induced ROS production and partially protects against apoptosis

Because iron chelators have been long suggested to protect against gentamicin-induced nephrotoxicity [33], we further tested deferoxamine,

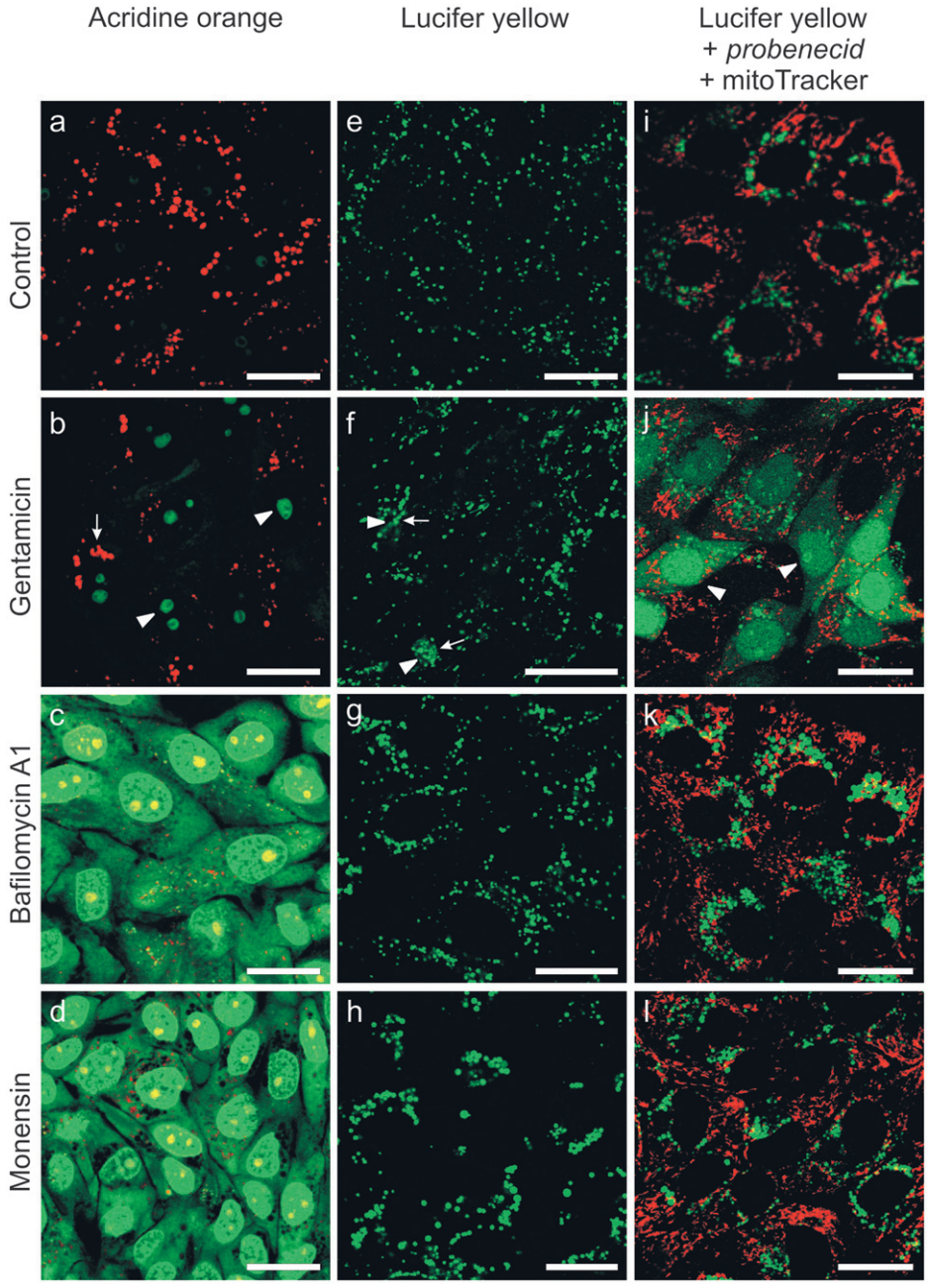

well-known to accumulate in lysosomes [34]. As shown in Fig. 5 left, treatment with 10 μM deferoxamine significantly decreased the production of ROS at all time points examined. Upon vital confocal imaging (Fig. 6), deferoxamine prevented gentamicin-induced ROS staining (below detection level), indicating that the iron chelator was acting on the gentamicin-induced lysosomal production of ROS. Deferoxamine also partially prevented apoptosis induced by gentamicin (Fig. 5; right). Increasing the concentration of deferoxamine to 25 μM caused cell toxicity (data not shown).

As for the antioxidants, deferoxamine did not decrease the cellular accumulation of gentamicin under the conditions used (22.3 ± 3 μg / mg protein after 48 h with 2 mM gentamicin alone *vs.* 25.9 ± 0.5 μg / mg protein in the presence of deferoxamine).

Deferoxamine and N-acetylcysteine do not protect against gentamicin-induced apoptosis when the drug is directly introduced in the cytosol by electroporation

To test whether the (partial) protection conferred by antioxidants was dependent from the lysosomal localization of gentamicin, the antibiotic was directly introduced in the cytosol by electroporation, thus by-passing the lysosomal compartment [12]. We previously reported that gentamicin triggers apoptosis at much lower concentrations when used in cells subjected to electroporation rather than when added to the culture medium. Therefore, cells were preincubated with deferoxamine or *N*-acetylcysteine, then electroporated with gentamicin and returned for 24 hours to gentamicin-free medium containing deferoxamine or *N*-acetylcysteine (Fig. 7). As predicted, whereas electroporation was innocuous (< 3% apoptotic nuclei) in the absence of gentamicin, electroporated cells were much more susceptible to gentamicin : 30% of apoptotic nuclei when the cells were electroporated at 0.1 mM *vs* 15% under endocytic uptake at 3 mM. Yet, deferoxamine or *N*-acetylcysteine were unable to confer any protection in electroporated cells, consistent with a role in lysosomes.

Discussion

Nephrotoxic drugs including aminoglycosides remain a major cause of acute renal failure in critically ill patients [35,36]. A large body of *in vitro* and *in vivo* evidence indicates that oxygen reactive species are important mediators of gentamicin nephrotoxicity [33,37]. Iron-gentamicin complex can increase reactive oxygen species [38,39] and a beneficial effect of ROS scavengers to protect against tubular necrosis induced by gentamicin in animals has been demonstrated [40]. The present study was carried out with LLC-PK1 cells, a model widely used for the study of various aspects of gentamicin-induced nephrotoxicity [41,42] and apoptosis [10,43] and extends over these observations demonstrating the role of ROS in the early signs of gentamicin cellular toxicity including lysosomal permeabilization, mitochondrial loss-of-function and apoptosis [44], and underlying the physiopathological role of lysosomes in this cascade.

The "lysosomal pathway of apoptosis" [15] proposes that cells can undergo apoptosis upon moderate lysosomal damage but will suffer necrosis if the damage is extensive [45,46]. The release of lysosomal constituents such as cathepsins could be sufficient to trigger apoptosis, since these enzymes can (i) cleave Bid, an antiapoptotic protein of the Bcl-2 family [47], (ii) directly activate pro-caspase-3 and −7 [48,49], and generate a cytochrome *c*-releasing factor from the cleavage of pro-caspase 2 [50]. The hypothesis that apoptosis can result from oxidative stress associated with lysosomal membrane permeabilization has been investigated since two decades, and led to emphasis on iron as a cause of generation of deleterious ROS (see [45] for review).

The data of the present report show that gentamicin induces ROS production very early on after cell exposure to the antibiotic, specifically in lysosomes (colocalization with Lysotracker), and can be partly prevented by experimental antioxidants or by the iron chelator used in clinical settings, deferoxamine. That lysosomal iron is a critical actor in gentamicin-induced early ROS production is supported by the following observations: (i) gentamicin starts accumulating in lysosomes [51]; (ii) lysosomes are organelles extremely active in redox reaction and containing significant amounts of transition metals, like iron [18]; and (iii) deferoxamine enters lysosomes by endocytosis [52] and can mobilize iron stores [34].

The use of H_2DCF to monitor ROS production fluorimetrically and morphologically does not provide direct information as to which type of ROS is being produced in lysosomes when cells are exposed to gentamicin. In the presence of iron and at acidic pH, H_2O_2 may form other reactive species such as $HO^{\cdot}$ and HO^{-} through the Fenton reaction [19]. Even more, oxidation of H_2DCF can be triggered without generation of ROS intermediates as described for hemoproteins like cytochrome c [53], nitric oxide [54], or pyocyanine [55]. H_2O_2 can be tentatively identified as one of the involved species because of protection by catalase against gentamicin-induced H_2DCF oxidation. Production of ROS in lysosomes upon gentamicin accumulation is critical, since addition of antioxidants or deferoxamine cannot protect against apoptosis when gentamicin is delivered directly in the cytosol by electroporation, thus by-passing lysosomes. Our observations thus lead to opposite conclusions than what has been derived from the effect of the acidotropic-sequestered detergent, MSDH on lysosomal and mitochondrial membranes permeabilization in which relocation to the cytosol of redox-active iron and cytochrome c has been considered responsible for H_2DCF oxidation [56]. The difference could possibly stem from the experimental systems with MSDH which has been reported to cause a massive disruption of lysosomes [11], whereas gentamicin led to a more subtle and slower lysosomal membrane permeabilization. In none of our conditions could detectable ROS production occur without being followed by significant increase in acridine orange release after > 2 h nor of apoptosis after > 1 day. However, this robust link in LLC-PK1 cells remains to be documented in vivo.

In vitro studies [21] show that ROS can be formed by aminoglycoside antibiotics in the presence of iron and polyunsaturated lipids, as electron donors. Phosphoinositides- or arachidonic-iron-gentamicin

Fig. 2. Subcellular localization of acridine orange and Lucifer yellow upon gentamicin *versus* bafilomycin A1 and monensin treatments. Acridine orange (a-d). Cells were preincubated with 5 μg/ml acridine orange for 15 min, then rinsed and replaced by culture medium supplemented with 10% foetal calf serum (control; a), or further treated with 3 mM gentamicin for 6 h (b), 100 nM bafilomycin A1 for 2 h to inhibit the vacuolar ATPase (c), or 50 μM monensin for 2 h to collapse proton gradients (d). Cells were briefly washed and immediately examined by vital imaging in the green and red channels simultaneously. Comparison of (a) with (b) suggests that gentamicin causes clustering of lysosomes (arrow). As to acridine orange redistribution, notice the modest green labeling of nucleoli upon gentamicin alone (arrowheads at b), contrasting with the strong green labeling in the entire cytosol and especially nucleosol in all cells upon lysosomal pH neutralization, with yellow signal indicating the higher nucleolar acridine orange concentration (c,d). Lucifer yellow (e-h). Cells were labelled with 2 mg/ml Lucifer yellow overnight (pulse), then chased for 6 hours in medium alone (e) or supplemented by 3 mM gentamicin (f), 100 nM bafilomycin A1 (g) or 50 μM monensin (h). Careful examination reveals at (f) a diffuse labeling (arrowheads) at the immediate vicinity of clustered lysosomes (arrows), but not upon lysosomal pH neutralization (g;h), suggesting lysosomal leakage of Lucifer yellow under gentamicin (for higher magnification and serial optical sectioning, see Suppl. Fig. 1). Sensitization of Lucifer yellow detection in the cytosol/nucleosol upon inhibition of organic anion transporters by probenecid (i-l). Cells were labeled with Lucifer yellow as above, except that pulse and chase were performed in the presence of 2.5 mM probenecid to sensitize detection of Lucifer yellow cytosolic release by preventing endosoma/ lysosomal recapture and/or cell expulsion by organic anion transporters. One hour before the end of chase, cells were further incubated for 30 min with MitoTracker red to simultaneously visualize mitochondria. After a final rinse, cells were immediately observed by confocal microscopy vital imaging, with sequential recording in the green (Lucifer yellow) and red (MitoTracker) channels. Notice the strong labeling of cytosol and especially nucleosol by Lucifer yellow in a large fraction of gentamicin-treated cells (j), but not upon lysosomal pH neutralizing agents (k;l). All scale bars, 20 μm.

ternary complexes [57] bring into a close proximity the redox center (Fe_{II}/Fe_{III}) and the electron donor [38]. This process is favored by acidic pH, the presence of reducing equivalents for generation of reactive hydroxyl radicals through the Fenton reaction [19], and low-molecular-weight iron, three conditions that are met in lysosomes [18,58,59]. Iron may, however, not be the only factor favouring the

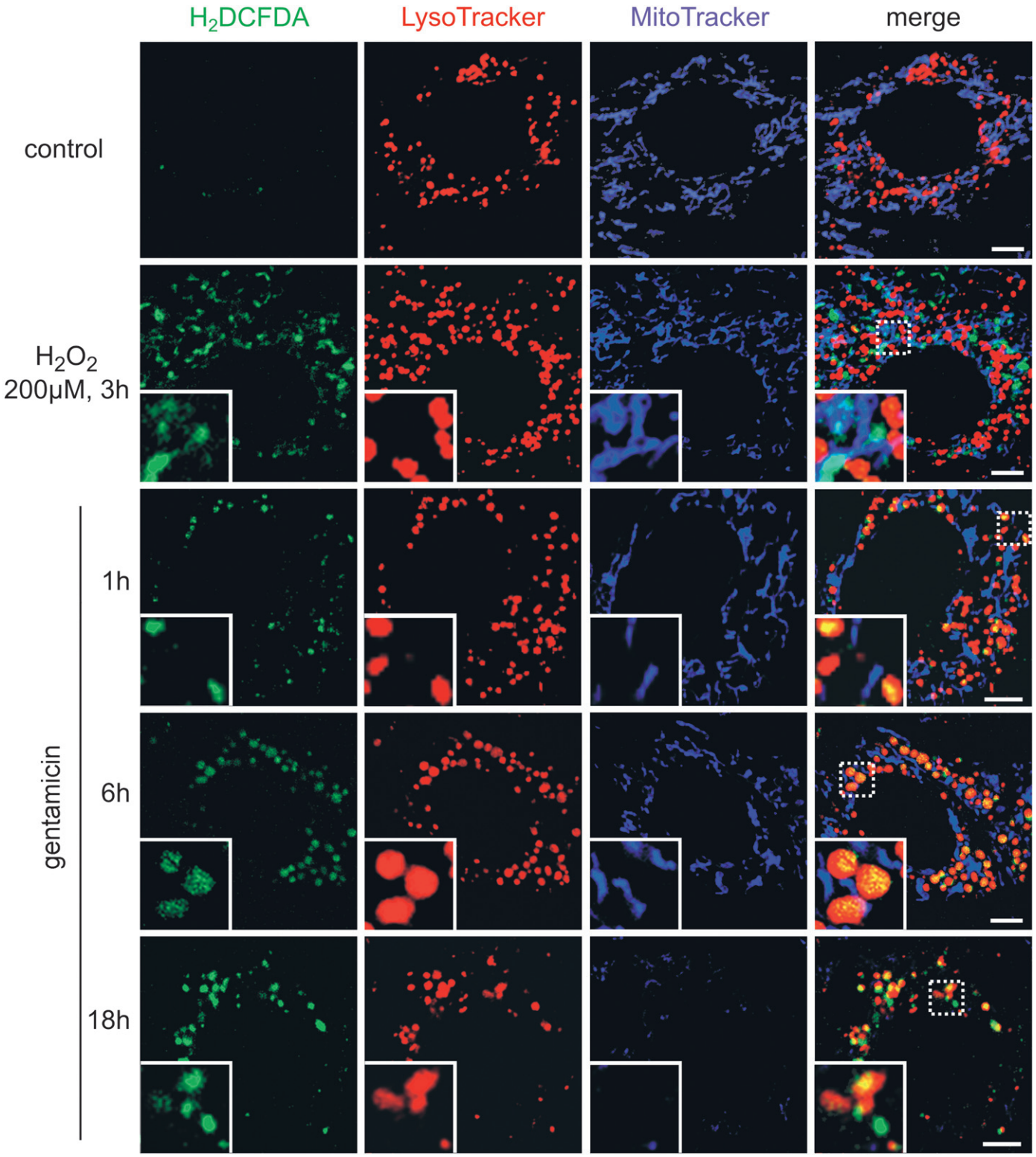

Fig. 3. Intracellular localization of ROS upon gentamicin and H_2O_2 treatments. Cells were kept untreated (control), or treated with either 200 µM H_2O_2 for 3 h or 2 mM gentamicin for the indicated times. One hour before the end of this incubation, cells were washed and sequentially incubated with MitoTracker for 30 min (to evidence mitochondria), then with a combination of LysoTracker (to detect lysosomes) and H_2DCFDA (to detect ROS production) for another 30 min, while maintaining the same concentrations of H_2O_2 or gentamicin. After washing, cells were immediately observed by confocal microscopy with sequential recording in the green (oxidized product of H_2DCF), red (LysoTracker) and blue (MitoTracker) channels. Merged images are shown at right. Background was set to the level of untreated cells. Upon H_2O_2 treatment, notice the complete dissociation of ROS from lysosomes, but its large codistribution with mitochondria. Upon gentamicin treatment, notice instead that ROS (green) fully overlap with LysoTracker (red) at 6 h, as obvious in the merge inset at the 4th row. All scale bars, 5 µm.

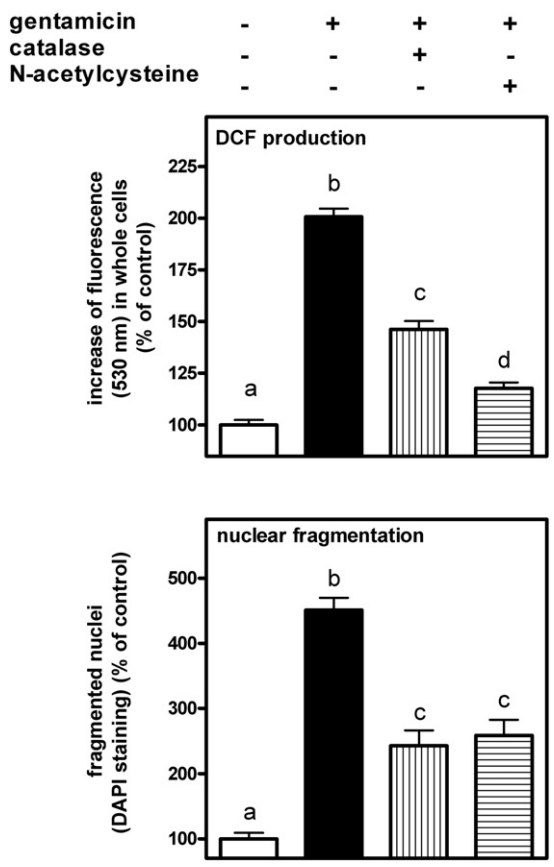

Fig. 4. Prevention by catalase and *N*-acetylcysteine of gentamicin-induced ROS production and apoptosis. Cells were preincubated for 3 h with 1,000 U/mL catalase or 1 mM *N*-acetylcysteine, then incubated with 2 mM gentamicin in the continued presence of catalase or *N*-acetylcysteine for 6 h (ROS) or 48 h (apoptosis). ROS production and apoptosis were measured as in Fig. 1. Data are expressed as percent of values in untreated cells (no gentamicin and no antioxidant; the addition of antioxidants alone had no effect) and are given as means ± SD (n = 6 from 2 separate experiments for ROS; n = 5 from 2 separate experiments for apoptosis). Statistical analysis: One-way analysis of variance and Tukey's Multiple comparison test; bars with different letters are significantly different from each other ($p<0.05$).

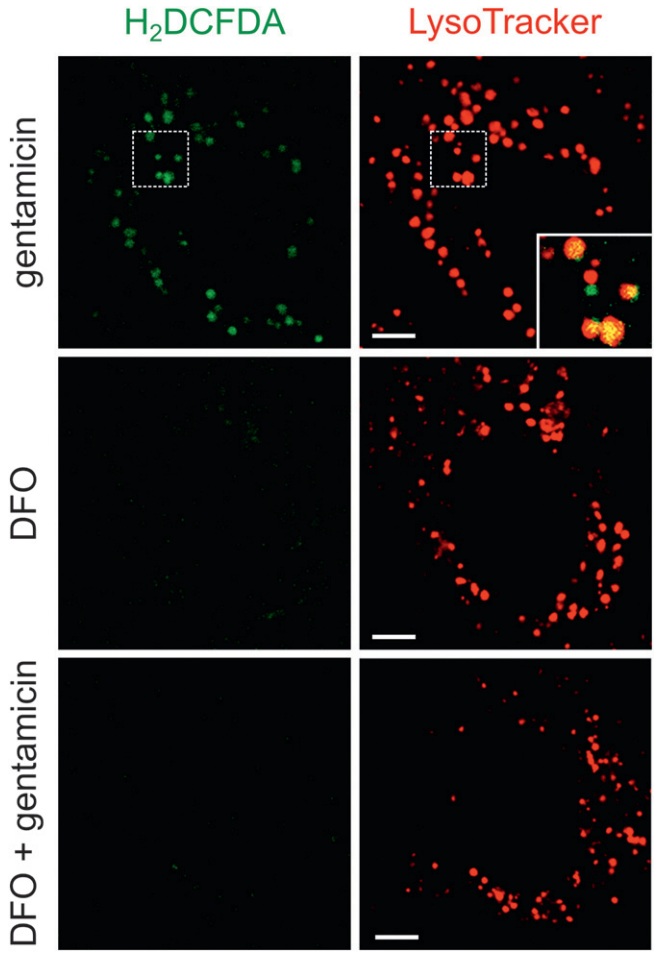

Fig. 6. Prevention by deferoxamine of gentamicin-induced ROS production in lysosomes. Cells were preincubated with 10 μM deferoxamine (DFO) for 3 h, then incubated with 2 mM gentamicin in the continued presence of deferoxamine (bottom row). Controls included cells exposed to gentamicin alone (upper row) or cells exposed to deferoxamine alone (middle row). Vital imaging was performed as in Fig. 3. All scale bars, 5 μm.

production of ROS, as deferoxamine afforded only a partial protective effect. Thus, while only iron-rich lysosomes would be amenable to protection by antioxidants and/or deferoxamine, those containing only negligible amounts of it, and for which labilization of membrane could occur through an iron-independent mechanism, would not be protected [60].

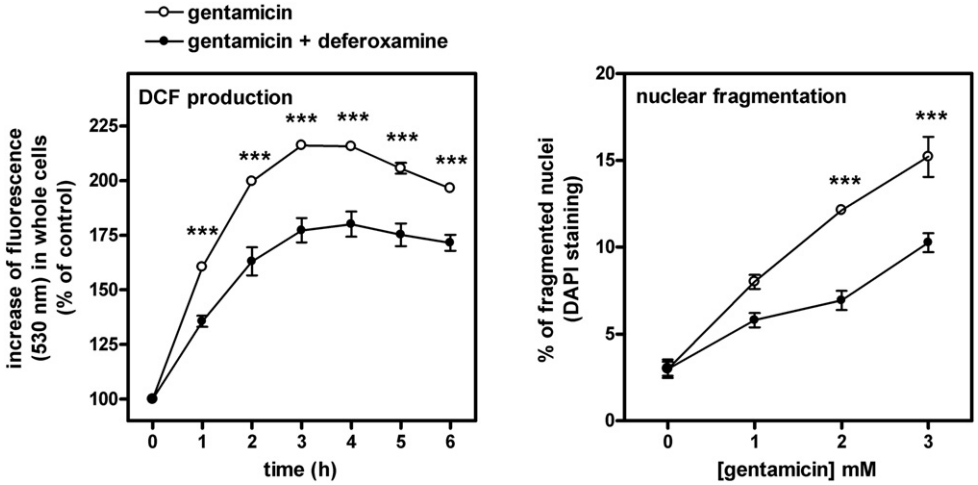

Fig. 5. Prevention by deferoxamine of gentamicin-induced ROS production and apoptosis. Cells were preincubated in the absence (open symbols) or presence (closed symbols) of 10 μM deferoxamine for 3 h, then exposed to gentamicin (2 mM) in the continued absence or the presence of deferoxamine for the indicated times (left) or gentamicin concentrations (right panel). ROS production and apoptosis were measured as in Fig. 1. Data are expressed as percentages of the values in untreated cells (no gentamicin and no deferoxamine; the addition of deferoxamine alone had no effect) and are given as means ± SD (n = 3). Where not visible, error bars are included in the symbols.

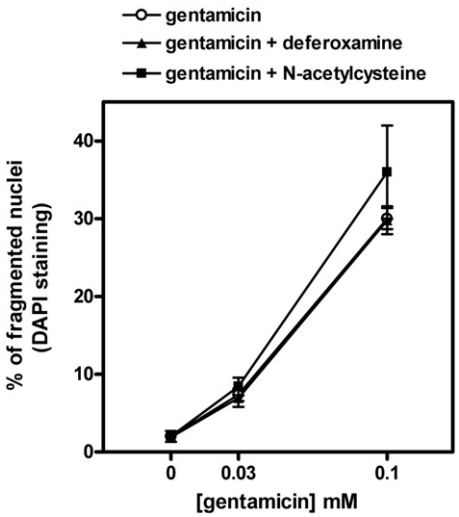

Fig. 7. Absence of protection by deferoxamine and *N*-acetylcysteine on apoptosis induced by gentamicin electroporation. Cells were preincubated or not with 10 μM deferoxamine or 1 mM *N*-acetylcysteine for 3 h, electroporated with gentamicin at the indicated concentrations, then returned for 24 h in gentamicin-free corresponding medium (deferoxamine or *N*-acetylcyteine, closed symbols; no further addition, open symbols). Apoptosis was measured as the percent cells with fragmented nuclei. Data are means ± SD (n = 3).

The generation of ROS caused by gentamicin may induce peroxidation of the lysosomal membranes and their permeabilization, as evidenced from studies using isolated lysosomes [61]. Acridine orange was often used as a probe for lysosomal membrane permeabilization. Arguably, the method does not allow to differentiate between (i) dilution upon release into the cytosol via membrane permeabilization, (ii) cytosolic dilution upon loss of lysosomal sequestration due to an oxidation of V-ATPase or ClC7, or (iii) alteration in emission spectrum of acridine orange, due to lysosomal alkalinization. However, while release and changes in lysosomal pH appear in parallel in cells upon photoactivation of the probe [62], studies using cultured proximal tubular cells failed to demonstrate an influence of gentamicin on lysosomal pH [63]. Moreover, cytosolic labeling of Lucifer yellow upon gentamicin treatment was clearly evidenced whereas it is completely absent upon changes in lysosomal pH induced by bafilomycin A1 or monensin.

ROS production in lysosomes seems to be a key pathogenic event for gentamicin toxicity leading to apoptosis. However, several data, including the partial protective effect afforded by *N*-acetylcysteine or deferoxamine and the incomplete correlation between the amount of ROS producted and the percentage of apoptotic cells detected at increasing concentrations of gentamicin, suggest that this mechanism is not the only one implicated in gentamicin-induced toxicity. It is well known that ultrafiltrated gentamicin is partially endocytosed by kidney epithelial cells lining the S1 and S2 segments of the proximal tubules where the drug enters by adsorptive/receptor mediated endocytosis after binding to acidic phospholipids and megalin respectively and eventually accumulates in lysosomes where it induces readily detectable phospholipidosis. However, and in contrast to fibroblasts and MDCK cells [10], only marginal phospholipidosis was found in LLC-PK1 cells, yet the level of apoptosis was similar in all three cell lines, suggesting that phospholipidosis is only one of the contributors of aminoglycoside toxicity at low therapeutic doses. The present paper depicts ROS generation selectively in lysosomes followed by lysosomal membrane permeabilization as a complementary mechanism for gentamicin-induced toxicity. One could tentatively reconcile these two mechanisms to account for the differential concentration dependence on ROS and apoptosis in LLC-PK1 cells, if ROS effects were maximal at a lower (~1 mM) extracellular gentamicin concentration and were synergized by a non-saturating concentration-dependent phospholipidosis, which develops as a slower process.

The clinical significance of our results remains to be evaluated. Although the extracellular concentrations of gentamicin used may seem overwhelming as compared to clinical serum concentrations, they were selected to match cellular concentrations reached in animals and humans treated with therapeutic doses (see discussion in [11]) and correspond to those eliciting apoptosis of proximal tubular cells in experimental animals [44]. Thus, ROS generation we evidenced may well occur *in vivo* under conditions pertinent of the clinical use of gentamicin. Moreover, the concentrations of *N*-acetylcysteine (1 mM) and of deferoxamine (10 μM) used to obtain a protective effect are in the range or below those observed in the serum of humans receiving intravenous therapeutic doses of these agents (0.2-3 mM for *N*-acetylcysteine [64]; up to 200 μM for deferoxamine [65]. Our results might therefore also have potential clinical implications in human aminoglycoside therapy; even if only partial cell protection can be reasonably expected, it could make a clear difference in overall clinical outcome.

In conclusion, ROS are rapidly produced in lysosomes of cultured LLC-PK1 cells incubated with gentamicin, and secondarily lead to lysosomal permeabilization followed by apoptosis. These effects can be largely prevented by preincubation with antioxidants or deferoxamine. Our data further point to lysosomal iron as a key actor in triggering the pathogenic cascade. Through the potential formation of a ternary complex gentamicin-iron-phosphoinositides, the accumulation of gentamicin *per se* is probably one of the critical event leading to lysosomal phospholipidosis, ROS production and lysosomal membrane permeabilization. We expect this study may help elucidate the subcellular mechanism responsible for activation of the lysosomal pathway of apoptosis and nephrotoxicity induced by aminoglycoside antibiotics, prompt further experimental work on the relation between permeabilization and apoptosis, and possibly justify clinical investigations.

Supplementary materials related to this article can be found online at doi:10.1016/j.freeradbiomed.2011.07.015.

Acknowledgments

FVB is Senior Research Associates of the Belgian *Fonds de la Recherche Scientifique* (F.R.S.-FNRS). This work was supported by the Walloon Region (NANOMEMB and DIANE centre of excellence programme), the F.R.S.-FNRS and the Université Catholique de Louvain (Fonds Spéciaux de Recherche and Actions de Recherche Concertées), Interuniversity Attraction Poles and EU VII (Eunefron).

References

[1] Mingeot-Leclercq, M. P.; Glupczynski, Y.; Tulkens, P. M. Aminoglycosides: activity and resistance. *Antimicrob. Agents Chemother.* **43:**727–737; 1999.
[2] Gilbert, D. N. Aminoglycosides. In: Mandell, G.L., Bennett, J.E., Dolin, R. (Eds.), Principles and Practice of Infectious Diseases. Elsevier/Churchill Livingstone, Philadelphia,pp. 328–356; 2005.
[3] Drusano, G. L.; Ambrose, P. G.; Bhavnani, S. M.; Bertino, J. S.; Nafziger, A. N.; Louie, A. Back to the future: using aminoglycosides again and how to dose them optimally. *Clin. Infect. Dis.* **45:**753–760; 2007.
[4] Durante-Mangoni, E.; Grammatikos, A.; Utili, R.; Falagas, M. E. Do we still need the aminoglycosides? *Int. J. Antimicrob. Agents* **33:**201–205; 2009.
[5] Sastrasinh, M.; Knauss, T. C.; Weinberg, J. M.; Humes, H. D. Identification of the aminoglycoside binding site in rat renal brush border membranes. *J. Pharmacol. Exp. Ther.* **222:**350–358; 1982.
[6] Moestrup, S. K.; Cui, S.; Vorum, H.; Bregengard, C.; Bjorn, S. E.; Norris, K.; Gliemann, J.; Christensen, E. I. Evidence that epithelial glycoprotein 330/megalin mediates uptake of polybasic drugs. *J. Clin. Invest* **96:**1404–1413; 1995.
[7] Giurgea-Marion, L.; Toubeau, G.; Laurent, G.; Heuson-Stiennon, J. A.; Tulkens, P. M. Impairment of lysosome-pinocytic vesicle fusion in rat kidney proximal tubules after treatment with gentamicin at low doses. *Toxicol. Appl. Pharmacol.* **86:** 271–285; 1986.
[8] Sandoval, R. M.; Molitoris, B. A. Gentamicin traffics retrograde through the secretory pathway and is released in the cytosol via the endoplasmic reticulum. *Am. J. Physiol. Ren. Physiol* **286:**F617–F624; 2004.
[9] Servais, H.; Ortiz, A.; Devuyst, O.; Denamur, S.; Tulkens, P. M.; Mingeot-Leclercq, M. P. Renal cell apoptosis induced by nephrotoxic drugs: cellular and molecular mechanisms and potential approaches to modulation. *Apoptosis* **13:**11–32; 2008.

[10] El Mouedden, M.; Laurent, G.; Mingeot-Leclercq, M. P.; Tulkens, P. M. Gentamicin-induced apoptosis in renal cell lines and embryonic rat fibroblasts. *Toxicol. Sci.* **56:** 229–239; 2000.

[11] Servais, H.; Van Der, S. P.; Thirion, G.; Van der, E. G.; Van Bambeke, F.; Tulkens, P. M.; Mingeot-Leclercq, M. P. Gentamicin-induced apoptosis in LLC-PK1 cells: involvement of lysosomes and mitochondria. *Toxicol. Appl. Pharmacol.* **206:**321–333; 2005.

[12] Servais, H.; Jossin, Y.; Van Bambeke, F.; Tulkens, P. M.; Mingeot-Leclercq, M. P. Gentamicin causes apoptosis at low concentrations in renal LLC-PK1 cells subjected to electroporation. *Antimicrob. Agents Chemother.* **50:**1213–1221; 2006.

[13] Mather, M.; Rottenberg, H. Polycations induce the release of soluble intermembrane mitochondrial proteins. *Biochim. Biophys. Acta* **1503:**357–368; 2001.

[14] Horibe, T.; Matsui, H.; Tanaka, M.; Nagai, H.; Yamaguchi, Y.; Kato, K.; Kikuchi, M. Gentamicin binds to the lectin site of calreticulin and inhibits its chaperone activity. *Biochem. Biophys. Res. Commun.* **323:**281–287; 2004.

[15] Guicciardi, M. E.; Leist, M.; Gores, G. J. Lysosomes in cell death. *Oncogene* **23:**2881–2890; 2004.

[16] Stoka, V.; Turk, V.; Turk, B. Lysosomal cysteine cathepsins: signaling pathways in apoptosis. *Biol. Chem.* **388:**555–560; 2007.

[17] Van Bambeke, F.; Mingeot-Leclercq, M. P.; Schanck, A.; Brasseur, R.; Tulkens, P. M. Alterations in membrane permeability induced by aminoglycoside antibiotics: studies on liposomes and cultured cells. *Eur. J. Pharmacol.* **247:**155–168; 1993.

[18] Yu, Z.; Persson, H. L.; Eaton, J. W.; Brunk, U. T. Intralysosomal iron: a major determinant of oxidant-induced cell death. *Free Radic. Biol. Med.* **34:**1243–1252; 2003.

[19] Baird, S. K.; Kurz, T.; Brunk, U. T. Metallothionein protects against oxidative stress-induced lysosomal destabilization. *Biochem. J.* **394:**275–283; 2006.

[20] Schafer, F. Q.; Buettner, G. R. Acidic pH amplifies iron-mediated lipid peroxidation in cells. *Free Radic. Biol. Med.* **28:**1175–1181; 2000.

[21] Lesniak, W.; Pecoraro, V. L.; Schacht, J. Ternary complexes of gentamicin with iron and lipid catalyze formation of reactive oxygen species. *Chem. Res. Toxicol.* **18:** 357–364; 2005.

[22] Sepulveda, F. V.; Burton, K. A.; Pearson, J. D. The development of gamma-glutamyltransferase in a pig renal-epithelial-cell line in vitro. Relationship to amino acid transport. *Biochem. J.* **208:**509–512; 1982.

[23] Hempel, S. L.; Buettner, G. R.; O'Malley, Y. Q.; Wessels, D. A.; Flaherty, D. M. Dihydrofluorescein diacetate is superior for detecting intracellular oxidants: comparison with 2',7'-dichlorodihydrofluorescein diacetate, 5(and 6)-carboxy-2',7'-dichlorodihydrofluorescein diacetate, and dihydrorhodamine 123. *Free Radic. Biol. Med.* **27:**146–159; 1999.

[24] Rundquist, I.; Olsson, M.; Brunk, U. Cytofluorometric quantitation of acridine orange uptake by cultured cells. *Acta Pathol. Microbiol. Immunol. Scand. A* **92:** 303–309; 1984.

[25] Nicolini, C.; Belmont, A.; Parodi, S.; Lessin, S.; Abraham, S. Mass action and acridine orange staining: static and flow cytofluorometry. *J. Histochem. Cytochem.* **27:** 102–113; 1979.

[26] Moriyama, Y.; Takano, T.; Ohkuma, S. Acridine orange as a fluorescent probe for lysosomal proton pump. *J. Biochem.* **92:**1333–1336; 1982.

[27] Steinberg, T. H.; Newman, A. S.; Swanson, J. A.; Silverstein, S. C. Macrophages possess probenecid-inhibitable organic anion transporters that remove fluorescent dyes from the cytoplasmic matrix. *J. Cell Biol.* **105:**2695–2702; 1987.

[28] Tulkens, P.; Trouet, A. The uptake and intracellular accumulation of aminoglycoside antibiotics in lysosomes of cultured rat fibroblasts. *Biochem. Pharmacol.* **27:** 415–424; 1978.

[29] Zdolsek, J. M.; Olsson, G. M.; Brunk, U. T. Photooxidative damage to lysosomes of cultured macrophages by acridine orange. *Photochem. Photobiol.* **51:**67–76; 1990.

[30] Steinberg, T. H.; Swanson, J. A.; Silverstein, S. C. A prelysosomal compartment sequesters membrane-impermeant fluorescent dyes from the cytoplasmic matrix of J774 macrophages. *J. Cell Biol.* **107:**887–896; 1988.

[31] Yoshimori, T.; Yamamoto, A.; Moriyama, Y.; Futai, M.; Tashiro, Y. Bafilomycin A1, a specific inhibitor of vacuolar-type H(+)-ATPase, inhibits acidification and protein degradation in lysosomes of cultured cells. *J. Biol. Chem.* **266:**17707–17712; 1991.

[32] Maxfield, F. R. Weak bases and ionophores rapidly and reversibly raise the pH of endocytic vesicles in cultured mouse fibroblasts. *J. Cell Biol.* **95:**676–681; 1982.

[33] Walker, P. D.; Shah, S. V. Evidence suggesting a role for hydroxyl radical in gentamicin-induced acute renal failure in rats. *J. Clin. Invest* **81:**334–341; 1988.

[34] Laub, R.; Schneider, Y. J.; Octave, J. N.; Trouet, A.; Crichton, R. R. Cellular pharmacology of deferrioxamine B and derivatives in cultured rat hepatocytes in relation to iron mobilization. *Biochem. Pharmacol.* **34:**1175–1183; 1985.

[35] Appel, G. B. Aminoglycoside nephrotoxicity. *Am. J. Med.* **88:**16S–20S; 1990.

[36] Pannu, N.; Nadim, M. K. An overview of drug-induced acute kidney injury. *Crit Care Med.* **36:**S216–S223; 2008.

[37] Walker, P. D.; Barri, Y.; Shah, S. V. Oxidant mechanisms in gentamicin nephrotoxicity. *Ren. Fail.* **21:**433–442; 1999.

[38] Priuska, E. M.; Schacht, J. Formation of free radicals by gentamicin and iron and evidence for an iron/gentamicin complex. *Biochem. Pharmacol.* **50:**1749–1752; 1995.

[39] Sha, S. H.; Schacht, J. Formation of reactive oxygen species following bioactivation of gentamicin. *Free Radic. Biol. Med.* **26:**341–347; 1999.

[40] Nakajima, T.; Hishida, A.; Kato, A. Mechanisms for protective effects of free radical scavengers on gentamicin-mediated nephropathy in rats. *Am. J. Physiol* **266:** F425–F431; 1994.

[41] Velasco-Velazquez, M. A.; Maldonado, P. D.; Barrera, D.; Torres, V.; Zentella-Dehesa, A.; Pedraza-Chaverri, J. Aged garlic extract induces proliferation and ameliorates gentamicin-induced toxicity in LLC-PK1 cells. *Phytother. Res.* **20:** 76–78; 2006.

[42] Steinmassl, D.; Pfaller, W.; Gstraunthaler, G.; Hoffmann, W. LLC-PK1 epithelia as a model for in vitro assessment of proximal tubular nephrotoxicity. *In Vitro Cell Dev. Biol. Anim* **31:**94–106; 1995.

[43] Choi, K. H.; Kim, T. I.; Chong, D. L.; Lee, H. Y.; Han, D. S. Gentamicin induced apoptosis of renal tubular epithelial (LLC-PK1) cells. *Korean J. Intern. Med.* **15:** 218–223; 2000.

[44] El Mouedden, M.; Laurent, G.; Mingeot-Leclercq, M. P.; Taper, H. S.; Cumps, J.; Tulkens, P. M. Apoptosis in renal proximal tubules of rats treated with low doses of aminoglycosides. *Antimicrob. Agents Chemother.* **44:**665–675; 2000.

[45] Kurz, T.; Terman, A.; Brunk, U. T. Autophagy, ageing and apoptosis: the role of oxidative stress and lysosomal iron. *Arch. Biochem. Biophys.* **462:**220–230; 2007.

[46] Turk, B.; Turk, V. Lysosomes as "suicide bags" in cell death: myth or reality? *J. Biol. Chem.* **284:**21783–21787; 2009.

[47] Stoka, V.; Turk, B.; Schendel, S. L.; Kim, T. H.; Cirman, T.; Snipas, S. J.; Ellerby, L. M.; Bredesen, D.; Freeze, H.; Abrahamson, M.; Bromme, D.; Krajewski, S.; Reed, J. C.; Yin, X. M.; Turk, V.; Salvesen, G. S. Lysosomal protease pathways to apoptosis. Cleavage of bid, not pro-caspases, is the most likely route. *J. Biol. Chem.* **276:** 3149–3157; 2001.

[48] Ishisaka, R.; Kanno, T.; Akiyama, J.; Yoshioka, T.; Utsumi, K.; Utsumi, T. Activation of caspase-3 by lysosomal cysteine proteases and its role in 2,2'-azobis-(2-amidinopropane)dihydrochloride (AAPH)-induced apoptosis in HL-60 cells. *J. Biochem.* **129:**35–41; 2001.

[49] Zhou, Q.; Salvesen, G. S. Activation of pro-caspase-7 by serine proteases includes a non-canonical specificity. *Biochem. J.* **324** (Pt 2)**:**361–364; 1997.

[50] Guicciardi, M. E.; Bronk, S. F.; Werneburg, N. W.; Yin, X. M.; Gores, G. J. Bid is upstream of lysosome-mediated caspase 2 activation in tumor necrosis factor alpha-induced hepatocyte apoptosis. *Gastroenterology* **129:**269–284; 2005.

[51] Silverblatt, F. J.; Kuehn, C. Autoradiography of gentamicin uptake by the rat proximal tubule cell. *Kidney Int.* **15:**335–345; 1979.

[52] Cable, H.; Lloyd, J. B. Cellular uptake and release of two contrasting iron chelators. *J. Pharm. Pharmacol.* **51:**131–134; 1999.

[53] Bromme, H. J.; Zuhlke, L.; Silber, R. E.; Simm, A. DCFH2 interactions with hydroxyl radicals and other oxidants–influence of organic solvents. *Exp. Gerontol.* **43:**638–644; 2008.

[54] Gunasekar, P. G.; Kanthasamy, A. G.; Borowitz, J. L.; Isom, G. E. NMDA receptor activation produces concurrent generation of nitric oxide and reactive oxygen species: implication for cell death. *J. Neurochem.* **65:**2016–2021; 1995.

[55] O'Malley, Y. Q.; Reszka, K. J.; Britigan, B. E. Direct oxidation of 2',7'-dichlorodihydrofluorescein by pyocyanin and other redox-active compounds independent of reactive oxygen species production. *Free Radic. Biol. Med.* **36:**90–100; 2004.

[56] Karlsson, M.; Kurz, T.; Brunk, U. T.; Nilsson, S. E.; Frennesson, C. I. What does the commonly used DCF test for oxidative stress really show? *Biochem. J.* **428:**183–190; 2010.

[57] Priuska, E.; Clark-Baldwin, K.; Pecoraro, V.; Schacht, J. NMR-studies of iron-gentamicin complexes and the implication for aminoglycoside toxicity. *Inorg. Chim. Acta* **273:**85–91; 1998.

[58] Ohkuma, S.; Poole, B. Fluorescence probe measurement of the intralysosomal pH in living cells and the perturbation of pH by various agents. *Proc. Natl Acad. Sci. USA* **75:**3327–3331; 1978.

[59] Pisoni, R. L.; Acker, T. L.; Lisowski, K. M.; Lemons, R. M.; Thoene, J. G. A cysteine-specific lysosomal transport system provides a major route for the delivery of thiol to human fibroblast lysosomes: possible role in supporting lysosomal proteolysis. *J. Cell Biol.* **110:**327–335; 1990.

[60] Nilsson, E.; Ghassemifar, R.; Brunk, U. T. Lysosomal heterogeneity between and within cells with respect to resistance against oxidative stress. *Histochem. J.* **29:** 857–865; 1997.

[61] Zdolsek, J.; Zhang, H.; Roberg, K.; Brunk, U. H2O2-mediated damage to lysosomal membranes of J-774 cells. *Free Radic. Res. Commun.* **18:**71–85; 1993.

[62] Olsson, G. M.; Rungby, J.; Rundquist, I.; Brunk, U. T. Evaluation of lysosomal stability in living cultured macrophages by cytofluorometry. Effect of silver lactate and hypotonic conditions. *Virchows Arch. B Cell Pathol. Incl. Mol. Pathol.* **56:** 263–269; 1989.

[63] Regec, A. L.; Trump, B. F.; Trifillis, A. L. Effect of gentamicin on the lysosomal system of cultured human proximal tubular cells. Endocytotic activity, lysosomal pH and membrane fragility. *Biochem. Pharmacol.* **38:**2527–2534; 1989.

[64] Prescott, L. F.; Donovan, J. W.; Jarvie, D. R.; Proudfoot, A. T. The disposition and kinetics of intravenous *N*-acetylcysteine in patients with paracetamol overdosage. *Eur. J. Clin. Pharmacol.* **37:**501–506; 1989.

[65] Miyazawa, K.; Ohyashiki, K.; Urabe, A.; Hata, T.; Nakao, S.; Ozawa, K.; Ishikawa, T.; Kato, J.; Tatsumi, Y.; Mori, H.; Kondo, M.; Taniguchi, J.; Tanii, H.; Rojkjaer, L.; Omine, M. A safety, pharmacokinetic and pharmacodynamic investigation of deferasirox (Exjade, ICL670) in patients with transfusion-dependent anemias and iron-overload: a Phase I study in Japan. *Int. J. Hematol.* **88:**73–81; 2008.